nature chemistry

ARTICLES

PUBLISHED ONLINE: 2 FEBRUARY 2015 | DOI: 10.1038/NCHEM.2160

Molecular length dictates the nature of charge carriers in single-molecule junctions of oxidized oligothiophenes

Emma J. Dell[1†], Brian Capozzi[2†], Jianlong Xia[1], Latha Venkataraman[2*] and Luis M. Campos[1*]

To develop advanced materials for electronic devices, it is of utmost importance to design organic building blocks with tunable functionality and to study their properties at the molecular level. For organic electronic and photovoltaic applications, the ability to vary the nature of charge carriers and so create either electron donors or acceptors is critical. Here we demonstrate that charge carriers in single-molecule junctions can be tuned within a family of molecules that contain electron-deficient thiophene-1,1-dioxide (TDO) building blocks. Oligomers of TDO were designed to increase electron affinity and maintain delocalized frontier orbitals while significantly decreasing the transport gap. Through thermopower measurements we show that the dominant charge carriers change from holes to electrons as the number of TDO units is increased. This results in a unique system in which the charge carrier depends on the backbone length, and provides a new means to tune p- and n-type transport in organic materials.

Organic electronic materials have impacted the development of semiconducting[1], photovoltaic[2] and thermoelectric devices[3,4]. The precise control afforded over molecular design by organic synthesis allows device properties to be tuned readily. For example, the ability to design and synthesize, from the principles of electronic structure, hole-/electron-transporting (p- and n-type, respectively) and ambipolar semiconductors has led to significant advancements in organic electronics[5–8]. Although design principles to create stable n-type organic materials are evolving, to isolate the intrinsic, fundamental electronic-structure contributions of the building blocks to bulk transport remains challenging. Strategies to increase electron affinity, such as incorporating electronegative functional groups onto conjugated molecules, have been developed to facilitate electron transport[9–11]. Although there is a wealth of organic electron-deficient building blocks that may be used to synthesize conjugated molecules[1,2], it is a challenge to predict a charge-carrier type prior to making the materials. For example, thiophene-1,1-dioxide (TDO, Fig. 1a), an oxidized counterpart of thiophene, is unique in that it imparts vastly different electronic properties that arise from the break in aromaticity when the sulfur lone pairs are engaged in bonding[12]. This leads to electron-deficient building blocks with strong dipole moments and oligoene-like backbones (Fig. 1b). Interestingly, compounds that contain TDO moieties have low-lying lowest unoccupied molecular orbitals (LUMOs) and n-type characteristics[11,13–17]. However, the point at which these materials exhibit n-type behaviour as a function of conjugation length is unknown. As families of n-type materials are under-developed in comparison to their p-type counterparts, to determine this crossover point is an important fundamental development that could lead to the design of advanced materials for applications in organic electronics[9,11].

To characterize electron-transport properties in these materials can be challenging because bulk transport depends on both intramolecular and intermolecular orbital coupling, the latter being a difficult parameter to control[11]. However, the scanning tunnelling microscope (STM)-based break-junction (STM-BJ) technique provides a means of probing the fundamental electronic properties at the single-molecule level, rather than in the bulk material (Fig. 1a)[18,19]. In this technique, a molecule is bridged between two nanoscale gold electrodes and its conductance is measured. The conductance depends on a number of factors, including the energetic alignment of the molecular frontier orbitals with the Fermi level of the gold electrodes. Whether the molecule conducts through the highest occupied molecular orbital (HOMO) or the LUMO depends on which of the two frontier orbitals is better aligned with the Fermi level and which is better coupled to the metal. Generally, the dominant factor in this alignment is the nature of the linker groups that bind to gold. For example, amine linker groups usually display HOMO conducting behaviour, whereas pyridine linkers display LUMO conducting behaviour[20,21]. At the molecular level, the nature of the charge carriers in single-molecule junctions can be evaluated by measuring the Seebeck coefficient (thermopower, S)[3,20]. The value of S relates to the derivative of the transmission function at the electrode Fermi energy (E_F)[22] and hence its sign relates to the nature of the charge carriers (Fig. 1c)[3,22].

Here we study the charge-transport characteristics of a family of molecules that are composed of electron-deficient oligo-TDO building blocks coupled to unoxidized thiophenes on both sides (Fig. 1a)[3,18,20]. This particular electron-rich/electron-poor combination yields a drastic reduction in the transport gap of these molecules (as compared to their all-thiophene counterparts). We show two interesting results that impact molecular conductance. First, the conductances exhibit a very shallow decay with molecular length (similar to that of oligoenes). This is a manifestation of their small energy gaps and very-well-conjugated backbones, with contributions from the quinoidal character of these systems. Second, through thermopower measurements with the two electrodes at different temperatures, we find that the dominant charge carriers switch from holes to electrons when the number of TDO monomers in the molecular backbone increases

[1]Department of Chemistry, Columbia University, New York 10027, USA. [2]Department of Applied Physics and Mathematics, Columbia University, New York 10027, USA. †Contributed equally to this work. *e-mail: lv2117@columbia.edu; lcampos@columbia.edu

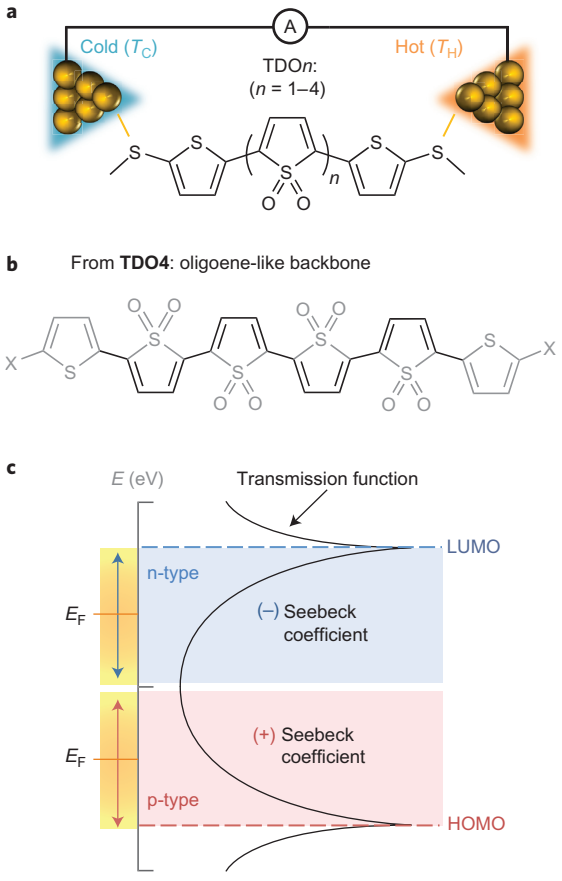

Figure 1 | Characterization of the nature of the charge carriers using the STM-BJ technique. a, Schematic representation of the STM-BJ set-up to measure the Seebeck coefficient of a family of molecules, TDO*n* (n = 1–4, **TDO4** is shown in the lower panel). The STM-BJ gold substrate is heated with the gold tip maintained at room temperature. **b**, Diagrammatic representation of the oligoene-like backbone in **TDO4** that results from the break in aromaticity of the thiophene ring on oxidation and therefore increases the conjugation along the backbone. **c**, Example of a transmission function that determines the probability that an electron of a given energy will tunnel through the molecular junction. Highlighted are sections in which E_F aligns closer to the HOMO or LUMO of the molecule. The Seebeck coefficient is proportional to the slope of the transmission function and thus yields positive or negative values depending on the alignment.

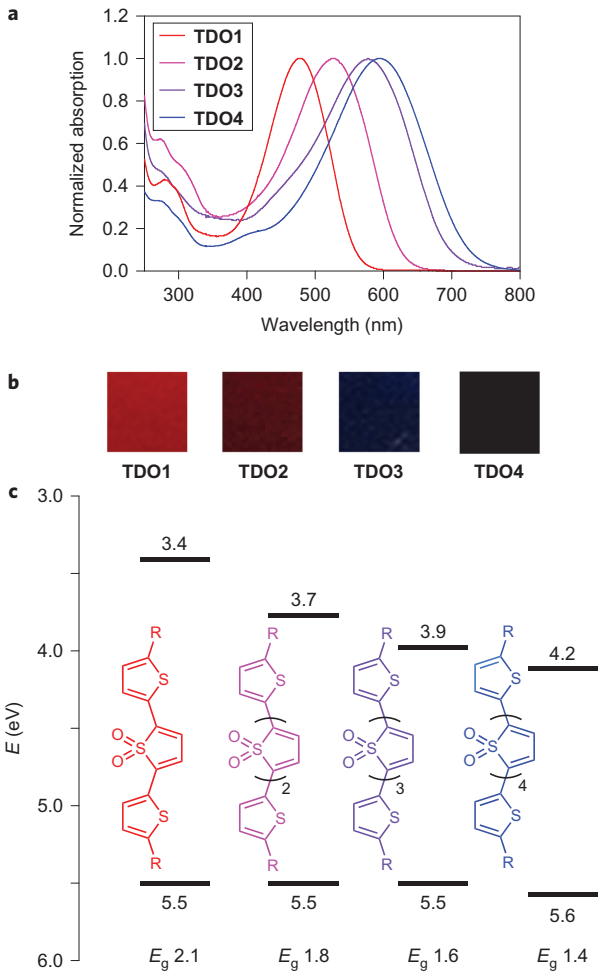

Figure 2 | Energy-level characterization of the TDO*n* family. a, Normalized UV-vis absorption spectra for the TDO*n* family measured in dichloromethane. **b**, Colour images of the 0.2 M TDO*n* dichloromethane solutions. **c**, CV-derived HOMO and LUMO levels (eV) and the HOMO–LUMO gap (E_g) for the TDO*n* family (R = SMe). These are determined by first measuring the oxidation and reduction potentials ($E_{ox1/2}$ and $E_{red1/2}$) by CV carried out in dichloromethane solutions using a Pt working electrode and an Ag/AgCl reference electrode (Supplementary Fig. 2 and Supplementary Table 1). The HOMO and LUMO levels for TDO*n* are then obtained using a HOMO level for ferrocene of –4.8 eV and $E_{ox1/2}$ 0.4 V (refs 24,42). The specific relationships used are: $E_{HOMO} = -e[E_{ox1/2} + 4.4]$ and $E_{LUMO} = -e[E_{red1/2} + 4.4]$.

with the linker groups remaining constant. This is the first time that changing the number of repeat units in an oligomer has been shown to change the conducting orbital, that is, the charge carriers. This work, therefore, provides an additional handle with which to tune conductance in single-molecule measurements, and also underlines the promise of TDO as a powerful electron-deficient motif with a low-lying LUMO to tune the electronic properties in bulk materials.

Results and discussion

Tuning the frontier molecular orbitals. We first show that our molecule design, which couples a central electron-deficient oligothiophene-1,1-dioxide section to two electron-rich thiophenes at either end, does, indeed, achieve a fully conjugated system with a small HOMO–LUMO gap[23]. To this end, we compared the ultraviolet–visible (UV-vis) absorption spectra of three different trimers: (1) a fully unoxidized (ter-thiophene) trimer, (2) a fully oxidized trimer and (3) a single-oxidized unit flanked by two gold-binding methyl-sulfide-bearing thiophenes[24], as shown in Supplementary Fig. 1. The fully unoxidized trimer has the shortest onset of absorption wavelength (λ_{onset} = 425 nm) and thus has the largest optical energy gap (see Supplementary Fig. 1). The fully oxidized non-aromatic trimer shows a significant red-shift (about 100 nm) at the onset of absorption. This is caused by a better electron delocalization along the molecular backbone, stabilization of the LUMO and increased planarity, which is inferred from the pronounced vibronic structure of its absorption spectrum[25]. The third trimer, **TDO1**, displays the longest λ_{onset} (575 nm), even though only a single unit is oxidized. This reduction in the optical gap of **TDO1** compared to that of the unoxidized trimer demonstrates the powerful donor–acceptor hybridization in these systems[26,27].

We now turn to UV-vis spectroscopy and cyclic voltammetry (CV) measurements to determine the trends in the frontier energy levels for the family of TDO*n* oligomers (with n = 1 to 4). The absorption spectra in Fig. 2a show a clear reduction in the

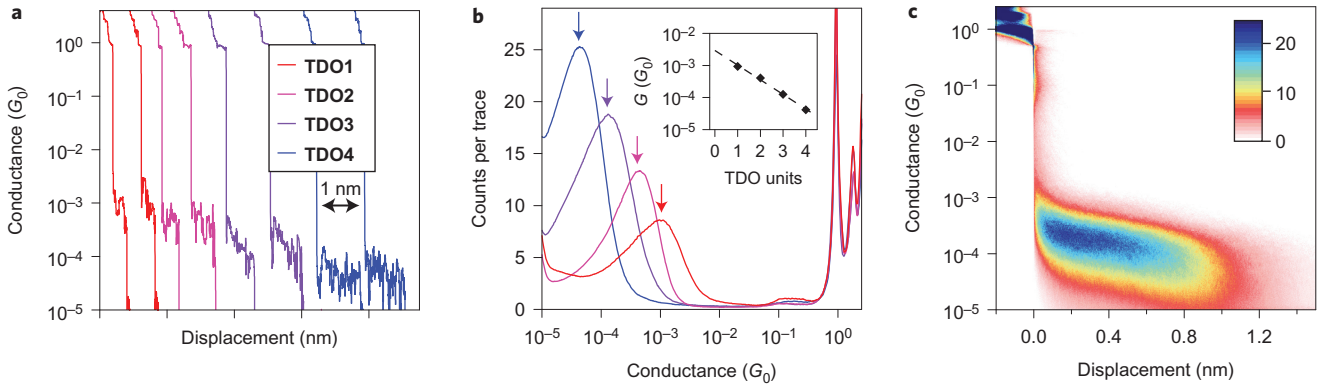

Figure 3 | Single-molecule conductance data. a, Sample conductance versus displacement traces, laterally offset, for the TDO*n* series. These traces display molecule-specific conductance features, which persist for longer displacements as the molecular length increases. **b**, 1D log-binned conductance histograms, each composed of 20,000 traces, for **TDO1–TDO4** measured at a 10 mV bias in 1-octylbenzene. Arrows indicate the peak-conductance positions. Inset: plot of the conductance as a function of the number of oxidized thiophene monomer units (n) in **TDO1–TDO4**. Using $G \approx e^{-\beta n}$, we obtained a decay constant of $1.04/n$. **c**, 2D conductance–displacement histogram for **TDO3** created by aligning all the traces at the point where the conductance crosses 0.5 G_0, and then overlaying them. The colour bar indicates the number of counts per 1,000 traces. For other 2D histograms see Supplementary Fig. 3.

optical gap with increasing n, accompanied by a deepening of the colours of the molecules in solution from red to dark blue, as shown in Fig. 2b. To understand how the gaps decrease, we looked at the CV measurements of the TDO*n* oligomers (Supplementary Fig. 2), which show both oxidation and reduction peaks, in contrast to the analogous series of all-unoxidized rings, in which only oxidation peaks are seen in the electrochemical window of the solvent[28]. The oxidation peaks for the TDO*n* family are around +1.1 V, indicating that the energy of the HOMO does not change significantly as additional TDO units are added. The reduction peaks, however, contain a shift from −1 V for **TDO1** to −0.3 V for **TDO4**, which shows that the LUMO energy decreases as TDO units are added. In Fig. 2c, we show the HOMO and LUMO levels derived from the CV data (see the Supplementary Information). We see that as the number of TDO repeat units increases, the LUMO of the molecules drops from 3.4 eV in **TDO1** to 4.1 eV in **TDO4** (Fig. 2c). The reduction potential for **TDO4** is similar to that of substituted fullerenes, which could imply an n-type behaviour[11,29], in stark contrast to the unoxidized oligothiophenes, which all demonstrate p-type characteristics[30]. Although these CV-derived values do not determine the exact alignment of the orbitals relative to a metal electrode[31], the trends should be discernible in transport measurements.

Conductance measurements. Next, we performed single-molecule conductance and thermopower measurements on the TDO*n* family to probe how their increased conjugation, smaller optical gaps and low-lying LUMOs impact charge transport through molecular junctions. For each molecule in the series, 20,000 conductance-versus-displacement traces were collected using the STM-BJ technique (Fig. 3a; see Methods and the Supplementary Information for details)[18,19]. All the measured conductance traces collected were compiled into one-dimensional (1D), logarithmically binned conductance histograms[32] (100 bins per decade) without data selection and are shown in Fig. 3b. These 1D histograms display a clear peak that yields the most-probable molecular conductance value, which decreases systematically with increasing numbers of TDO monomers (n) (Fig. 3b). The relatively narrow breadth of the conductance histogram peaks is indicative of a rather rigid backbone in this class of molecules[28,33]. A 2D histogram for **TDO3** that retains the displacement information and is created from the same data (Fig. 3c) shows that these junctions sustain a 1 nm elongation. Comparing 2D histograms across the series (Supplementary Fig. 3) we see a clear increase in the molecular plateau length with increasing backbone length. This indicates that we have probed similar junction structures for all the molecules in this series[34]. The inset of Fig. 3b shows the peak conductance values on a semilogarithmic scale plotted against n and illustrates that the conductance decreases exponentially with increasing n ($G \approx e^{-\beta n}$) with a decay constant of $\beta = 1.04/n$. As these TDO units are non-aromatic, the conduction path follows that of a chain of alternating double and single bonds across the backbone, as shown in Fig. 1b. We therefore used a through-bond distance of 5.4 Å n^{-1} as opposed to a through-space distance of 3.8 Å n^{-1} to convert the measured β into a decay constant of 0.2 Å^{-1}. Interestingly, this value compares well with β determined for oligoene systems[35,36], and shows that transport across TDO oligomers is similar to that across alkene oligomers.

Thermopower measurements. Although the narrow HOMO–LUMO gap of the isolated molecules is reflected in the relatively high conductances and shallow decay of the TDO*n* series, small-bias conductance measurements alone do not provide any information on the nature of the orbital that dominates charge transport. To probe how such an orbital alignment is impacted by the dramatic lowering of the LUMO with an increasing number of oxidized thiophene units, we measured the Seebeck coefficient of these molecular junctions. The Seebeck coefficient for a single-molecule junction is determined by heating the substrate although the STM tip kept at room temperature and measuring the thermoelectric current with no external bias voltage applied (Fig. 1a, see Methods and the Supplementary Information for details)[20]. With the molecular conductance (G), thermoelectric current (I) and temperature difference (ΔT) known for each junction measured, S is given by $S = I/(G\Delta T)$ (ref. 22). We compiled the Seebeck coefficients from hundreds of junctions for each molecule into the histograms shown in Fig. 4a; these were then fitted with a Gaussian function to determine the most-frequently measured Seebeck coefficient for each molecule.

In Fig. 4b we plot the Seebeck coefficient versus the molecular length. For **TDO1–TDO3**, this value is positive and decreases non-linearly with length, whereas for **TDO4** it is negative and relatively large in magnitude. This trend is contrary to that observed in amine-, thiol- and trimethyltin-linked oligophenyl series, in which the Seebeck coefficient maintains the same sign (positive) and increases in magnitude with molecular length[3,21,37]. Such measurements

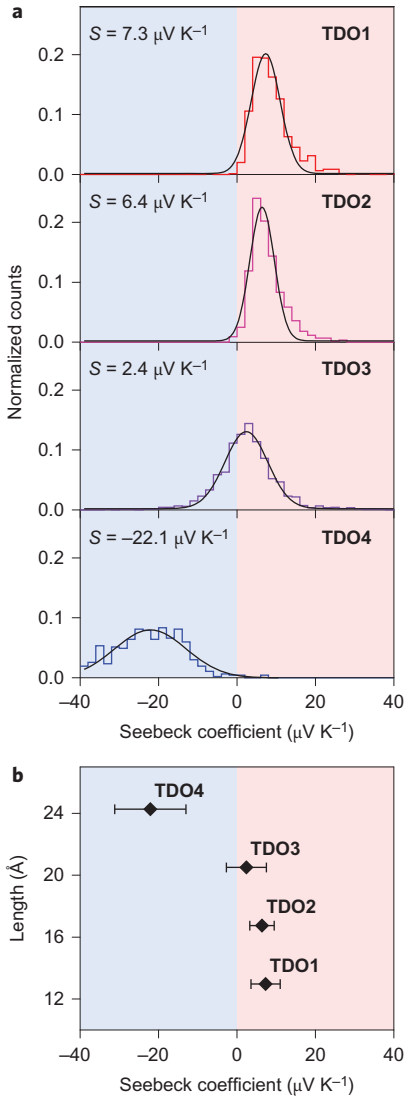

Figure 4 | Single-molecule thermopower data. a, STM-BJ measurements taken with a temperature difference of 16 K between the gold tip and the substrate. While the molecule bridges the gap between the electrodes, the applied bias voltage is dropped to zero and the thermoelectric current is measured. Seebeck coefficients for each junction are then calculated using this current, as detailed in the text and Supplementary Information, and compiled into the 1D histograms shown. The black curves are Gaussian fits to the Seebeck coefficient distributions. **b**, Plot of Seebeck coefficients as a function of molecular length for the TDO*n* family with error bars that reflect the error in the Gaussian fits. A shift from positive to negative Seebeck values with increasing length is seen, which indicates a change in the charge carriers from holes to electrons.

demonstrate that these oligophenyls conduct via hole transport through the HOMO. The increase in magnitude of S with increasing length in these oligophenyls is attributed to the HOMO moving closer to E_F and simultaneously narrowing as the conducting orbital delocalizes over a longer molecule, which results in a larger slope in the transmission function at E_F. Based on our measurements on the TDO*n* series, we infer that transport in **TDO1** is dominated by HOMO, which indicates a hole-type transport. Using the conductance and Seebeck coefficient determined for **TDO1** and assuming the line shape of a single-Lorentzian transmission function, we found that the conducting orbital was −2 eV from E_F, in agreement with results from current and voltage (IV) measurements for **TDO1** (Supplementary Fig. 7, and the discussion in the Supplementary Information).

The large, negative Seebeck coefficient measured for **TDO4** indicates that electron transport is dominated by the LUMO. The magnitude of this value is comparable to that of C_{60}, which is among the highest values of organic compounds[38]. Again, assuming a single-Lorentzian transmission function for this system, we infer that the LUMO is 0.7 eV from E_F, consistent with results from IV measurements (Supplementary Fig. 7). The Seebeck coefficient for **TDO2** is smaller in magnitude than that for **TDO1**; if the transport in **TDO2** was dominated by the HOMO, we would expect a larger Seebeck coefficient compared to that of **TDO1**. We thus conclude that the transport in **TDO2** is not dominated by a single orbital. Finally, the slightly positive but small-magnitude Seebeck coefficient measured for **TDO3** suggests that the E_F lies in a relatively flat region of the transmission function, possibly in the middle of the HOMO–LUMO gap with both orbitals contributing to the charge transport. This implies that the transmission functions for both **TDO2** and **TDO3** do not follow a Lorentzian shape and, thus, a direct determination of the level alignment for these two systems is not possible with these measurements. Taken together, these measurements show that contributions from the LUMO to charge transport become increasingly more important as the number of oxidized thiophene units in the molecular backbone increases. We showed additional evidence of a change in the conducting orbital by carrying out solvent-dependent measurements[39] on **TDO1** and **TDO4** (see Supplementary Fig. 6 for details). This trend is in accord with the previously discussed UV-vis and CV measurements, in which a decreasing optical gap and a lowering of the reduction potential are observed with increasing molecular length (Fig. 2).

Interestingly, despite changing the conducting orbital, we still found an exponential dependence of conductance on molecular length with a well-defined decay constant. To understand how we could observe this, we turned to an n-site tight-binding model in which each site is assigned an occupied and an unoccupied orbital (Supplementary Fig. 8). This model is described in detail in the Supplementary Information. In general, we found that the conductance decays exponentially, as long as E_F is not close to any resonance, even with a change in the dominant transport channel with increasing length. However, for longer chain lengths, we saw a deviation from this exponential dependence if an orbital was closer to E_F.

We have used STM-BJ conductance and Seebeck-coefficient measurements to illustrate the transport characteristics of molecules that contain TDO, a poorly studied building block that has tremendous impact on the electronic properties of both polymers and small molecules. Our findings demonstrate that these molecules constitute a unique system in which the charge carrier in gold–molecule–gold junctions switches from holes to electrons with an increasing number of monomers. Although previous studies showed that the dominant conducting orbital is generally dictated by the gold-binding linker units[20], control through the backbone length is unprecedented. Moreover, **TDO4** is shown to have a relatively high Seebeck coefficient[20,38], which suggests that these systems may be potential candidates for thermoelectric devices. The conductance data also show that the transport properties of oligo-TDOs are similar to those of oligoalkenes, reinforcing the fully conjugated and non-aromatic nature of their backbones. These studies demonstrate that small changes in molecular structure can have a major impact on charge-transport characteristics—a strategic molecular design provides a method for engineering the carrier type in molecular devices. Additionally, as the oxidized thiophene units have a dramatic impact on the LUMO, these studies reveal a potentially new family of building blocks for n-type materials.

Methods

This section describes key experiments only; an extended experimental section is provided in the Supplementary Methods.

Synthesis of the TDO*n* family. The general procedure to synthesize these molecules is as follows (see the Supplementary Information for details). First, a dibromo-terminated oligothiophene was treated with Rozen's reagent[40]. Rozen's reagent is a stabilized form of hypofluorous acid that can be used to oxidize the thiophene units. Then, a Stille coupling was performed to add the gold-binding linkers (with a flanking unoxidized thiophene moiety) to the oxidized thiophene oligomers[41]. As an example, the synthesis of **TDO1** is described here. A mixture of 40 ml acetonitrile and 4 ml water was cooled to −10°C. A mixture of 20% F_2 in N_2 was bubbled through this solution for an hour to generate HOF·CH_3CN (Rozen's reagent). A 1 ml aliquot was removed, added to a saturated KI solution and the liberated I_2 was titrated against $Na_2S_2O_3$ to determine the concentration of Rozen's reagent. 2,5-Dibromothiophene (400 mg, 1.65 mmol, 1 equiv.) was dissolved in 10 ml CH_2Cl_2 and cooled to 0 °C. HOF·CH_3CN (55 ml, 0.15 M, 8.27 mmol, 5 equiv.) was added dropwise and the solution was stirred at room temperature for two hours (for each oxidation, 2–3 equiv. Rozen's reagent per thiophene moiety were used). The reaction was quenched by adding a saturated $NaHCO_3$ solution dropwise. After a standard aqueous workup, 2,5-dibromothiophene-1,1-dioxide was obtained in 78% yield. Next, 2,5-dibromothiophene-1,1-dioxide (30 mg, 0.11 mmol, 1 equiv.) and tetrakis(triphenylphosphine)palladium (6.4 mg, 0.0055 mmol, 0.05 equiv.) were dissolved in 2 ml dimethylformamide and sparged with Ar for 20 minutes. 2-Tributylstannyl-5-thiomethylthiophene (92 mg, 0.22 mmol, 2 equiv.) was added and the solution was stirred at 80 °C for five hours. Standard aqueous work up and column chromatography yielded a deep reddish bronze solid, **TDO1**, in 71% yield.

Conductance measurements. Conductance measurements were performed using the STM-BJ technique with a home-built modified STM, described in detail previously[19]. Conductance data were collected by driving a mechanically cut gold tip into and out of contact with a gold-on-mica substrate (100 nm 99.995% Au, thermally evaporated). As the tip was retracted at a speed of 16 nm s^{-1}, the resulting gold junction thinned down to a gold single-atom contact, which ruptured on further elongation. After rupture, a molecule may bridge the gap and, because we simultaneously measured current (I) and voltage (V), we could determine the molecular junction conductance ($G = I/V$). For these measurements, TDO*n* molecules were introduced in a 1-octylbenzene solution (concentrations of 10 μM to 1 mM). For each molecule, 20,000 conductance verses displacement traces were collected at an applied bias of 10 mV; these traces were then used (without selection) to construct conductance histograms.

Seebeck-coefficient measurements. We determined the Seebeck coefficient of single molecules by performing break-junction measurements with an applied temperature gradient and a zero applied bias voltage. Data were collected using a slightly modified procedure of the break-junction technique, as detailed previously[20]. Briefly, a peltier was used to heat the gold-on-mica substrate with the tip kept near room temperature. All the temperatures were measured using a thermocouple. A modified piezo ramp was applied, as detailed in the Supplementary Information and shown in Supplementary Fig. 4. Thousands of traces were collected when a 0 K and 16 K temperature difference was applied between the tip and the substrate. Selected traces that evidenced a molecular junction were analysed to determine the thermoelectric current across the molecule at zero applied bias. This current was used to determine the Seebeck coefficient for the molecule in the junction. Histograms of the measured thermoelectric currents are shown in Supplementary Fig. 5.

Received 17 September 2014; accepted 12 December 2014; published online 2 February 2015

References

1. Heeger, A. J. Semiconducting and metallic polymers: the fourth generation of polymeric materials (Nobel lecture). *Angew. Chem. Int. Ed.* **40,** 2591–2611 (2001).
2. Henson, Z. B., Mullen, K. & Bazan, G. C. Design strategies for organic semiconductors beyond the molecular formula. *Nature Chem.* **4,** 699–704 (2012).
3. Reddy, P., Jang, S. Y., Segalman, R. A. & Majumdar, A. Thermoelectricity in molecular junctions. *Science* **315,** 1568–1571 (2007).
4. Bubnova, O. *et al.* Semi-metallic polymers. *Nature Mater.* **13,** 190–194 (2014).
5. Schwartz, G. *et al.* Flexible polymer transistors with high pressure sensitivity for application in electronic skin and health monitoring. *Nature Commun.* **4,** 1859 (2013).
6. You, J. *et al.* A polymer tandem solar cell with 10.6% power conversion efficiency. *Nature Commun.* **4,** 1446 (2013).
7. Gustafsson, G. *et al.* Flexible light-emitting diodes made from soluble conducting polymers. *Nature* **357,** 477–479 (1992).
8. Meijer, E. J. *et al.* Solution-processed ambipolar organic field-effect transistors and inverters. *Nature Mater.* **2,** 678–682 (2003).
9. Facchetti, A., Mushrush, M., Katz, H. E. & Marks, T. J. n-type building blocks for organic electronics: a homologous family of fluorocarbon-substituted thiophene oligomers with high carrier mobility. *Adv. Mater.* **15,** 33–38 (2003).
10. Katz, H. E. *et al.* A soluble and air-stable organic semiconductor with high electron mobility. *Nature* **404,** 478–481 (2000).
11. Anthony, J. E., Facchetti, A., Heeney, M., Marder, S. R. & Zhan, X. W. n-type organic semiconductors in organic electronics. *Adv. Mater.* **22,** 3876–3892 (2010).
12. Chen, W. *et al.* Aromaticity decreases single-molecule junction conductance. *J. Am. Chem. Soc.* **136,** 918–920 (2014).
13. Barbarella, G., Pudova, O., Arbizzani, C., Mastragostino, M. & Bongini, A. Oligothiophene-*S*,*S*-dioxides: a new class of thiophene-based materials. *J. Org. Chem.* **63,** 1742–1745 (1998).
14. Camaioni, N., Ridolfi, G., Fattori, V., Favaretto, L. & Barbarella, G. Oligothiophene-*S*,*S*-dioxides as a class of electron-acceptor materials for organic photovoltaics. *Appl. Phys. Lett.* **84,** 1901–1903 (2004).
15. Wei, S. *et al.* Bandgap engineering through controlled oxidation of polythiophenes. *Angew. Chem. Int. Ed.* **53,** 1832–1836 (2014).
16. Potash, S. & Rozen, S. New conjugated oligothiophenes containing the unique arrangement of internal adjacent [all]-*S*,*S*-oxygenated thiophene fragments. *Chem. Eur. J.* **19,** 5289–5296 (2013).
17. Dell, E. J. & Campos, L. M. The preparation of thiophene-*S*,*S*-dioxides and their role in organic electronics. *J. Mater. Chem.* **22,** 12945–12952 (2012).
18. Xu, B. Q. & Tao, N. J. J. Measurement of single-molecule resistance by repeated formation of molecular junctions. *Science* **301,** 1221–1223 (2003).
19. Venkataraman, L. *et al.* Single-molecule circuits with well-defined molecular conductance. *Nano Lett.* **6,** 458–462 (2006).
20. Widawsky, J. R., Darancet, P., Neaton, J. B. & Venkataraman, L. Simultaneous determination of conductance and thermopower of single molecule junctions. *Nano Lett.* **12,** 354–358 (2012).
21. Malen, J. A. *et al.* Identifying the length dependence of orbital alignment and contact coupling in molecular heterojunctions. *Nano Lett.* **9,** 1164–1169 (2009).
22. Paulsson, M. & Datta, S. Thermoelectric effect in molecular electronics. *Phys. Rev. B* **67,** 241403 (2003).
23. Yu, G., Gao, J., Hummelen, J. C., Wudl, F. & Heeger, A. J. Polymer photovoltaic cells—enhanced efficiencies via a network of internal donor–acceptor heterojunctions. *Science* **270,** 1789–1791 (1995).
24. Park, Y. S. *et al.* Contact chemistry and single-molecule conductance: a comparison of phosphines, methyl sulfides, and amines. *J. Am. Chem. Soc.* **129,** 15768–15769 (2007).
25. Amir, E. *et al.* Synthesis and characterization of soluble low-bandgap oligothiophene-[all]-*S*,*S*-dioxides-based conjugated oligomers and polymers. *J. Polym. Chem. A* **49,** 1933–1941 (2011).
26. Sonar, P., Williams, E. L., Singh, S. P. & Dodabalapur, A. Thiophene–benzothiadiazole–thiophene (D-A-D) based polymers: effect of donor/acceptor moieties adjacent to D-A-D segment on photophysical and photovoltaic properties. *J. Mater. Chem.* **21,** 10532–10541 (2011).
27. Bolivar-Marinez, L. E., dos Santos, M. C. & Galvao, D. S. Electronic structure of push–pull molecules based on thiophene oligomers. *J. Phys. Chem.* **100,** 11029–11032 (1996).
28. Capozzi, B. *et al.* Length-dependent conductance of oligothiophenes. *J. Am. Chem. Soc.* **136,** 10486–10492 (2014).
29. Yee, S. K., Malen, J. A., Majumdar, A. & Segalman, R. A. Thermoelectricity in fullerene-metal heterojunctions. *Nano Lett.* **11,** 4089–4094 (2011).
30. Sirringhaus, H. *et al.* Two-dimensional charge transport in self-organized, high-mobility conjugated polymers. *Nature* **401,** 685–688 (1999).
31. Bredas, J-L. Mind the gap! *Mater. Horiz.* **1,** 17–19 (2014).
32. Gonzalez, M. T. *et al.* Electrical conductance of molecular junctions by a robust statistical analysis. *Nano Lett.* **6,** 2238–2242 (2006).
33. Dell, E. J. *et al.* Impact of molecular symmetry on single-molecule conductance. *J. Am. Chem. Soc.* **135,** 11724–11727 (2013).
34. Kamenetska, M. *et al.* Formation and evolution of single-molecule junctions. *Phys. Rev. Lett.* **102,** 126803 (2009).
35. Visoly-Fisher, I. *et al.* Conductance of a biomolecular wire. *Proc. Natl Acad. Sci. USA* **103,** 8686–8690 (2006).
36. Meisner, J. S. *et al.* A single-molecule potentiometer. *Nano Lett.* **11,** 1575–1579 (2011).
37. Widawsky, J. R. *et al.* Length-dependent thermopower of highly conducting Au–C bonded single molecule junctions. *Nano Lett.* **13,** 2889–2894 (2013).
38. Evangeli, C. *et al.* Engineering the thermopower of C60 molecular junctions. *Nano Lett.* **13,** 2141–2145 (2013).
39. Fatemi, V., Kamenetska, M., Neaton, J. B. & Venkataraman, L. Environmental control of single-molecule junction transport. *Nano Lett.* **11,** 1988–1992 (2011).

40. Rozen, S. HOF·CH_3CN: probably the best oxygen transfer agent organic chemistry has to offer. *Acc. Chem. Res.* **47,** 2378–2389 (2014).
41. Stille, J. K. The palladium-catalyzed cross-coupling reactions of organotin reagents with organic electrophiles. *Angew. Chem. Int. Ed. Engl.* **25,** 508–523 (1986).
42. Bredas, J. L., Silbey, R., Boudreaux, D. S. & Chance, R. R. Chain-length dependence of electronic and electrochemical properties of conjugated systems: polyacetylene, polyphenylene, polythiophene, and polypyrrole. *J. Am. Chem. Soc.* **105,** 6555–6559 (1983).

Acknowledgements

This work was supported primarily by the National Science Foundation under award DMR-1206202. E.J.D. thanks the Howard Hughes Medical Institute, American Australian Association and Dow Chemical Company for International Research Fellowships.

Author contributions

B.C., E.J.D., L.V. and L.M.C. conceived and designed the experiments. B.C. performed the conductance and thermopower measurements. E.J.D. and J.X. synthesized and characterized the molecules. All authors discussed the results. E.J.D. and B.C. contributed equally to this work. E.J.D., B.C., L.V. and L.M.C. wrote the paper with contributions from all authors.

Additional information

Supplementary information and chemical compound information are available in the online version of the paper. Reprints and permissions information is available online at www.nature.com/reprints. Correspondence and requests for materials should be addressed to L.V. and L.M.C.

Competing financial interests

The authors declare no competing financial interests.